THE ALOHA ACCESS (UWB)^2 PROTOCOL REVISITED FOR IEEE 802.15.4A

Maria-Gabriella Di Benedetto, Luca De Nardis,
Guerino Giancola, Daniele Domenicali

School of Engineering
University of Rome La Sapienza

The IEEE 802.15.4a Task Group recently proposed Impulse Radio Ultra Wide Band (IR-UWB) for a physical layer that can provide combined communication and ranging in low data rate indoor/outdoor networks. At present, it is therefore particularly relevant to design IEEE 802.15.4a MAC strategies that are appropriately tailored on the physical layer. Previously, we proposed the Uncoordinated Baseborn Wireless medium access control for UWB networks (UWB)^2, a UWB-tailored MAC based on the low probability of pulse collision. The (UWB)^2 adopted the Aloha principle and enabled location-based network optimization by providing and storing estimates of distance between nodes. This paper first revisits the (UWB)^2 MAC protocol in view of its application to IEEE 802.15.4a. The structure of both control and data MAC protocol data units is defined based on the legacy 802.15.4 MAC in order to allow a seamless support, for both centralized and distributed network topologies, as defined in the parent standard. Secondly, this work extends and completes the analysis of (UWB)^2 since it takes into account multipath-prone channels. Channel parameters, for both indoor and outdoor propagation scenarios in Line Of Sight (LOS) and Non-Line Of Sight (NLOS) conditions, were derived from the channel model defined within the 802.15.4a channel sub-committee.
Results highlight that the (UWB)^2 protocol is robust to multipath, and provides high throughput and low delay, with performance scaling gracefully as a function of the number of users and the user bit rate. Results confirm and support the adoption of (UWB)^2 principles for low data rate UWB communications.

Index Terms - Ultra Wide Band, MAC, Low Data Rate

1. INTRODUCTION

Low data rate and low cost networks for mixed indoor/outdoor communications are of great interest in sensor and ad-hoc networking. The interest towards low data rate networks led in 2003 to the definition of the IEEE 802.15.4 standard for low rate, low complexity, and low power wireless networks [1]. The 802.15.4 standard also forms the basis of the ZigBee technology, which provides a comprehensive solution for low data rate networking from physical layer to applications [2].

Both IEEE 802.15.4 and ZigBee lack, however, an important requirement of forthcoming low data rate systems, namely, the capability of locating, with sufficiently high precision, objects and individuals by means of distributed, infrastructure-independent positioning algorithms.

The introduction of positioning in low data rate networks is a top priority of the recently formed IEEE 802.15.4a Task Group [3], which recently proposed Impulse Radio Ultra Wide Band (IR-UWB) as an attractive transmission technique for indoor and outdoor low data rate wireless networks [4], [5]. Thanks to its ultra wide bandwidth that spans over several GHz, IR-UWB has some interesting properties, in particular:

- an inherently high temporal resolution that provides good robustness in the presence of multipath, thereby allowing communication despite obstacles and Non-Line-Of-Sight (NLOS) propagation conditions.
- the capability of providing accurate ranging, thanks to its high temporal resolution. Distance information can then be used for deriving the physical position of terminals in the network.

The definition of the Uncoordinated Baseborn Wireless medium access control for UWB networks $(UWB)^2$ protocol was based on the above specific features of IR-UWB [6]. $(UWB)^2$ also evaluates and stores distances, which are then used by positioning and routing algorithms. The $(UWB)^2$ approach for propagation over AWGN channels was validated in [7].

In the present work, we revisit $(UWB)^2$ by redefining the structure of both control and DATA MAC Protocol Data Units (MACPDUs) based on the PDU structure of the original IEEE 802.15.4 MAC standard in order to guarantee compatibility of the new MAC protocol with both distributed and centralized network topologies defined in the 802.15.4 standard.

Next, we extend the analysis of the $(UWB)^2$ protocol to the case of multipath-affected channels, for both indoor and outdoor channel scenarios in Line Of Sight (LOS) and Non-Line Of Sight (NLOS) conditions. Channel parameters were obtained from the channel model proposed within the 802.15.4a Task Group, and a set of channel realizations were considered for each selected scenario.

Finally, Multi User Interference (MUI) was also included in the performance analysis based on an enhanced version of the Pulse Collision model specific for IR-UWB [7], which takes into account multipath. This MUI model is used to analyze performance of $(UWB)^2$ by simulation, as a function of channel, network size, and user bit rates.

The paper is organized as follows: Section 2 summarizes $(UWB)^2$ and the ranging scheme, and Section 3 defines the format of the $(UWB)^2$ MAC Protocol Data Unit, based on the structure defined within the preexisting 802.15.4 MAC. The Pulse Collision MUI model is introduced in Section 4. Performance evaluation of $(UWB)^2$ in presence of multipath and MUI for different number of users and offered traffic is carried out in Section 5. Section 6 draws conclusions.

2. THE $(UWB)^2$ MAC PROTOCOL

The high temporal resolution of IR-UWB signals has the beneficial side effect of reinforcing robustness to MUI, in particular for low data rate applications [4]. As a consequence, access to the medium in low data rate UWB networks can be based on a most straightforward solution, Aloha ([8], [6]), by which devices transmit in an uncoordinated fashion. Thanks to the resilience to MUI offered by impulse radio, correct reception

for multiple simultaneous links can be obtained. An Aloha-like approach may also favor lowering costs, since it does not rely on specific physical layer (PHY) functions, such as carrier sensing, and may thus be adapted with little effort to different PHYs.

As for the duty cycle of emitted signals, low data rate scenarios usually lead to an average Pulse Repetition Period (PRP), the average time between two consecutive pulses emitted by a device, on the order of $10^{-4} \div 10^{-5}$ s, with an average duration of emitted pulses typically on the order of 10^{-10} s. Theoretically, the duty cycle can thus be as low as 10^{-6}. However, a detailed analysis of this issue requires introducing the channel model in order to take into account propagation effects on pulse duration. When Time Hopping (TH) is the selected coding technique, TH – Code Division Multiple Access (TH-CDMA) is a natural choice for multiple access. The adoption of TH-CDMA can introduce an additional degree of freedom, since the effect of pulse collisions is further reduced by the adoption of different codes on different links. Two factors cooperate in determining the robustness to MUI: low duty cycle of emitted signals, and association of different TH-Codes with different links.

$(UWB)^2$ is a multi-channel MAC protocol that is based on the combination of Aloha with TH-CDMA [6]. $(UWB)^2$ adopts the combination of a common code for signaling, where terminals share the same code, and code collisions are avoided thanks to phase shifts between different links, and Transmitter codes for data transfers, where each terminal has a unique code for transmitting, and the receiver switches to the code of the transmitter for receiving a packet.

The packet exchange between transmitter TX and receiver RX that takes place during connection set-up may also serve for enabling a simple ranging procedure, based on a three-way exchange. During set-up, TX and RX prepare a DATA packet transmission by exchanging a Link Establishment (LE) packet transmitted on the Common Code, followed by a Link Confirm (LC) packet transmitted on the Transmitter Code of RX, and finally by the DATA packet on the Transmitter Code of TX. This handshake allows storing distance between TX and RX at both TX and RX. The protocol also foresees the presence of a procedure by which each terminal *i* maintains a ranging database for all neighboring terminals. Each entry of the database contains the ID *j* of the neighbor, the estimated distance to *j*, and a timestamp indicating the time at which the estimation was performed.

3. THE $(UWB)^2$ MACPDU FORMAT

The format of the MACPDU originally proposed in [6] was revisited and modified in order to take into account the characteristics of the future IEEE 802.15.4a PHY.

The MACPDU is composed of a header, a payload, and a trailer. The standard header, shared by all PDUs and long up to 23 bytes, is derived from the 802.15.4 header and is organized as follows:

- frame control (2 bytes)
- equence number (1 byte)
- destination PAN identifier (2 bytes)
- destination address (2/8 bytes)
- source PAN identifier (2 bytes)
- source address (2/8 bytes)

In the case of LE control packets (link set-up phase of $(UWB)^2$), the header includes the following additional fields:

- Time Hopping flag (1 bit), used to inform destination whether the standard Time Hopping code or a different one is going to be adopted in the DATA transmission;
- Time Hopping code (0/2 bytes), used for communicating the TH code to the destination (e.g., by including the code identifier, assuming that all nodes share a common codebook).

In the case of DATA PDU, the header contains the 1 byte additional field N_{PDU} that indicates to the destination the number of additional DATA PDUs that will be sent from the source. If N_{PDU} is different from 0, the destination will keep on

listening on the DATA TH code and wait for additional DATA PDUs. The length of the payload is set to 0 for LE and LC PDUs, while the ACK PDU has a 2 byte payload containing the status of the corresponding DATA PDU. Finally, DATA PDUs have a payload length of up to 103 bytes.

All PDUs include a 2 byte trailer consisting of a CRC code evaluated on the entire PDU.

The above PDU structure leads to a maximum PDU length of 129 bytes, corresponding to the case of a DATA PDU with full header (24 bytes), full payload (103 bytes), and the 2 byte trailer.

4. BER EVALUATION UNDER THE PULSE COLLISION MODEL

4.1. System model

We assume IR-UWB transmissions with Pulse Position Modulation (PPM) and TH coding. Signals generated at TX are described as follows:

$$s_{TX}(t) = \sqrt{E_{TX}} \sum_j p_0\left(t - jT_S - \theta_j - \varepsilon b_{\lfloor j/N_S \rfloor}\right), \quad (1)$$

where $p_0(t)$ is the energy-normalized waveform of the transmitted pulses, E_{TX} is the transmitted energy per pulse, T_S is the average pulse repetition period, $0 \le \theta_j < T_S$ is the TH time shift of the j-th pulse, ε is the PPM shift, b_x is the x-th bit of a binary source sequence $\mathbf{b}$, N_S is the number of pulses transmitted for each bit, and $\lfloor x \rfloor$ is the inferior integer part of x.

Propagation for link m occurs over a multipath-affected channel with impulse response given by:

$$h^{(m)}(t) = X^{(m)} \sum_{l=0}^{L^{(m)}} \sum_{k=0}^{K} \alpha_{k,l}^{(m)} \delta\left(t - \Delta t^{(m)} - T_l^{(m)} - \tau_{k,l}^{(m)}\right), \quad (2)$$

where $X^{(m)}$ is the amplitude gain, $L^{(m)}$ is the number of clusters, K is the number of paths that are considered within each cluster, $\delta(t)$ is the Dirac function, $\Delta t^{(m)}$ is the propagation delay, $T_l^{(m)}$ is the delay of the l-th cluster with respect to $\Delta t^{(m)}$, $\tau_{k,l}^{(m)}$ is the delay of the k-th path relative to the l-th cluster arrival time, and $\alpha_{k,l}^{(m)}$ is the real-valued tap weight of the k-th path within the l-th cluster. Tap weights are energy-normalized and thus verify:

$$\sum_{l=0}^{L^{(m)}} \sum_{k=0}^{K} \left(\alpha_{k,l}^{(m)}\right)^2 = 1, \quad (3)$$

For all channel parameters in (2), we adopt the statistical characterization that is suggested in [10] for 9 different propagation environments, i.e., *i*) residential LOS, *ii*) residential NLOS, *iii*) office LOS, *iv*) office NLOS, *v*) outdoor LOS, *vi*) outdoor NLOS, *vii*) industrial LOS, *viii*) industrial NLOS, and *ix*) open outdoor environment NLOS (farm, snow-covered open area).

For link m, both channel gain $X^{(m)}$ and propagation delay $\Delta t^{(m)}$ depend on distance of propagation $D^{(m)}$ between TX and RX. For $X^{(m)}$, in particular, one has:

$$X^{(m)} = 1 \Big/ \sqrt{10^{\left(PL^{(m)}/10\right)}}, \quad (4)$$

where $PL^{(m)}$ is the path loss in dB, which can be modelled as indicated in [10].

Reference TX and RX are assumed to be perfectly synchronized. The channel output is corrupted by thermal noise and MUI generated by N_i interfering and asynchronous IR-UWB devices. The received signal at RX input writes:

$$s_{RX}(t) = r_u(t) + r_{mui}(t) + n(t), \quad (5)$$

where $r_u(t)$, $r_{mui}(t)$, and $n(t)$ are the useful signal, MUI, and thermal Gaussian noise with double-sided power spectral density $N_0/2$, respectively. By denoting as 0 the reference link between TX and RX, the useful signal $r_u(t)$ writes as follows:

$$r_u(t) = \sqrt{E_0} \sum_j \sum_{l=0}^{L^{(0)}} \sum_{k=0}^{K} \alpha_{k,l}^{(0)} \cdot \cdot p_0\left(t - jT_S - \theta_j^{(0)} - \varepsilon b_{\lfloor j/N_S \rfloor} - \Delta t^{(0)} - T_l^{(0)} - \tau_{k,l}^{(0)}\right), \quad (6)$$

where $E_0 = (X^{(0)})^2 E_{TX}$ is the total received energy per pulse.

As for $r_{mui}(t)$, we assume all interfering signals to be characterized by the same T_S; thus:

$$r_{mui}(t) = \sum_{n=1}^{N_i} \sqrt{E_n} \sum_j \sum_{l=0}^{L^{(n)}} \sum_{k=0}^{K} \alpha_{k,l}^{(n)} \cdot \cdot p_0\left(t - jT_S - \theta_j^{(n)} - \varepsilon b_{\left\lfloor j/N_S^{(n)} \right\rfloor}^{(n)} - \Delta t^{(n)} - T_l^{(n)} - \tau_{k,l}^{(n)}\right), \quad (7)$$

where index n represents the wireless link between the nth interfering device and RX. In (7), $E_n = (X^{(n)})^2 E_{TX}$, and $\Delta\tau^{(n)}$ are the received energy per pulse and the delay for link n. The terms $\theta_j^{(n)}$, $b_x^{(n)}$ and $N_S^{(n)}$ in (7) are the time shift of the j-th pulse for user n, the x-th bit, and the number of pulses per bit, respectively for user n.

Both TH codes and data bit sequences are assumed to be randomly generated and correspond to pseudonoise sequences, that is, $\theta_j^{(n)}$ terms are assumed to be independent random variables uniformly distributed in the range $[0,T_S)$, and $b_x^{(n)}$ values are assumed to be independent random variables with equal probability to be "0" or "1." Based on the above assumptions, the N_i relative delays $\Delta\tau^{(0)}$–$\Delta\tau^{(n)}$, with $n = 1,...,N_i$ may be reasonably modelled as independent random variables uniformly distributed between 0 and T_S.

As well known, the optimum receiver structure for (6) consists of a RAKE receiver composed of a parallel bank of correlators, followed by a combiner that determines the variable to be used for the decision on the transmitted symbol. Each correlator of the RAKE is locked on one of the different replicas of the transmitted waveform $p_0(t)$. The complexity of such a receiver increases with the number of multipath components that are analyzed and combined before decision, and can be reduced by processing only a sub-set of the components that are available at the receiver input [4].

Such a reduction, however, entails a decrease in the available useful energy in the decision process, together with a consequent decrease in receiver performance. As a result, system designers have the possibility to trade the cost of the devices with the performance of the physical layer. For some application scenarios, for example, it might be better to have very cheap devices with modest performance with respect to high-priced terminals with better performance. In the examined scenario, we adopt a basic IR receiver that analyzes a single component of the received signal. This basic receiver is composed by a coherent correlator followed by an ML detector [4]. In every bit period, the correlator converts the received signal in (5) into a decision variable Z that forms the input of the detector. Soft decision detection is performed. For each pulse, we assume that the correlator locks onto the multipath component with maximum energy. By indicating with l_M and k_M the cluster and the path of the maximum energy multipath component for the reference user, the input of the detector Z for a generic bit b_x is as follows:

$$Z = \int_{xN_ST_S + \Delta T^{(0)}}^{(x+1)N_ST_S + \Delta T^{(0)}} s_{RX}(t)\, m_x\left(t - \Delta T^{(0)}\right) dt \quad (8)$$

where

$$\Delta T^{(0)} = \Delta t^{(0)} + T_{l_M}^{(0)} + \tau_{k_M, l_M}^{(0)} \quad (9)$$

and where

$$m_x(t) = \sum_{j=xN_S}^{(x+1)N_S} \left(p_0\left(t - jT_S - \theta_j\right) - p_0\left(t - jT_S - \theta_j - \varepsilon\right)\right) \quad (10)$$

By introducing (5) into (8), we obtain: $Z = Z_u + Z_{mui} + Z_n$, where Z_u is the signal term, Z_{mui} is the MUI contribution, and Z_n is the noise contribution, which is Gaussian with zero mean and variance $\sigma_n^2 = N_S N_0 \xi(\varepsilon)$, where $\xi(\varepsilon) = 1 - R_0(\varepsilon)$, and where $R_0(\varepsilon)$ is the autocorrelation function of the pulse waveform $p_0(t)$ [4]. Bit b_x is estimated by comparing the Z term in (8) with a zero-valued threshold according to the following rule: when Z is positive decision is "0", when Z is negative decision is "1."

4.2. BER estimation under the Pulse Collision approach

According to Section 4.1, the average probability of error on the bit at the output of the detector for independent and equiprobable

transmitted bits is: BER = $Prob\{Z<0|b_x=0\} = Prob\{Z_{mui}<-y\}$, where $y = Z_u+Z_n$ is a Gaussian random variable with mean:

$$\mu_y = N_S\xi(\varepsilon)\sqrt{\left(\alpha^{(0)}_{l_M,k_M}\right)^2 E_0} = N_S\xi(\varepsilon)\sqrt{E_u} \qquad (11)$$

and variance $\sigma_y^2 = N_S N_0 \xi(\varepsilon)$. The quantity E_u in (11) indicates the amount of useful energy conveyed by the maximum multipath contribution. The average BER at the receiver output can be evaluated by applying the Pulse Collision (PC) approach [11]. First, we compute the conditional BER for a generic y value, i.e., $Prob\{Z_{mui} < -y \mid y\}$, and we then average over all possible y values, that is:

$$\text{BER} = \int_{-\infty}^{+\infty} Prob\{Z_{mui} < -y \mid y\}\, p_Y(y)\, dy \qquad (12)$$

Next, we expand the conditional BER in order to take into account collisions between pulses of different transmissions. In a bit period, the number of possible collisions at the input of the reference receiver, denoted with c, is confined between 0 and $N_S N_i$, with N_S pulses per bit and N_i interfering users. Thus:

$$\text{BER} = \sum_{c=0}^{N_S N_i} P_C(c) \int_{-\infty}^{+\infty} Prob\{\, Z_{mui} < -y \mid y, c\,\}\, p_Y(y)\, dy \qquad (13)$$

where P_C (c) is the probability of having c collisions at the receiver input. For independent interferers, P_C (c) can be expressed through the binomial distribution:

$$P_C(c) = \binom{N_S N_i}{c} (P_0)^c (1-P_0)^{N_S N_i - c}, \qquad (14)$$

where P_0 is the basic collision probability, which is defined as the probability that an interfering device produces a non-zero contribution within a single T_S. Given the receiver structure in (8), we approximate P_0 as follows:

$$P_0 = \frac{T_m + \varepsilon + \tau_{MAX}}{T_S}. \qquad (15)$$

where T_m is the time duration of the pulse waveform $p_0(t)$, and τ_{MAX} is the maximum among the values of the root mean square delay spread for the N_i channels between the interfering devices and RX. Note that (15) provides acceptable P_0 values if $T_S > T_m + \varepsilon + \tau_{MAX}$, which is reasonable for LDR systems with long pulse repetition periods. This condition guarantees that no Inter Frame Interference (ISI) is present at the receiver, even in the presence of multipath propagation.

As regards $Prob(Z_{mui} < -y \mid y,c)$, we adopt the linear model introduced in [11], that is:

$$Prob\left(Z_{mui} < -y \mid y, c\right) = \begin{cases} 1 & \text{for} \quad y \le -\zeta(n) \\ 1 - \dfrac{P_C(c)}{2}\left(1 + \dfrac{y}{\zeta(c)}\right) & \text{for} \quad \zeta(n) < y \le 0 \\ \dfrac{P_C(c)}{2}\left(1 - \dfrac{y}{\zeta(c)}\right) & \text{for} \quad 0 < y \le \zeta(n) \\ 0 & \text{for} \quad y > \zeta(n), \end{cases} \qquad (16)$$

where $\zeta(c)$ indicates the maximum interference contribution that can be measured at the output of the correlator. Based on [11], we propose here the following approximation for ζ(c):

$$\zeta(c) = \sum_{j=1}^{N_i} \left(\left\lceil \frac{c-j+1}{N_i} \right\rceil \sqrt{E_{\text{int}}^{(j)} \frac{T_m + \varepsilon}{\tau_{rms}^{(j)}}} \right) \qquad (17)$$

where $\{E_{int}^{(1)}, E_{int}^{(2)}, \ldots, E_{int}^{(Ni)}\}$ are the interfering energies $\{E_1, E_2, \ldots, E_{Ni}\}$ of (7), sorted in descending order so that $E_{int}^{(j)} \ge E_{int}^{(j+1)}$ for $j = 1,\ldots,N_i$-1. The expression in (17) indicates that the value of the maximum interference contribution at the receiver output is computed privileging dominating interferers, that is, those users with the highest interfering energies.

Note that in (17) we multiply the value of jth interfering energy $E_{int}^{(j)}$ by $(T_m+\varepsilon)/\tau_{rms}^{(j)}$.

This operation indicates that only part of the energy associated with a colliding pulse contributes to Z in (8), corresponding to the ratio between the correlator window $T_m+\varepsilon$ and the length of the pulse at the receiver, approximated by $\tau_{rms}^{(j)}$. By combining

(16) into (13), one has:

$$\mathrm{BER} \approx \frac{1}{2} erfc\left(\sqrt{\frac{1}{2}\frac{N_S E_u}{\mathrm{N}_0}\xi(\varepsilon)}\right) + \sum_{c=0}^{N_f N_S} \frac{P_C(c)^2}{2}\Omega\left(\frac{N_S E_u}{\mathrm{N}_0}\xi(\varepsilon), \frac{\varsigma(c)^2}{N_S \mathrm{N}_0 \xi(\varepsilon)}\right) , \quad (18)$$

where

$$\Omega(A,B) = \frac{1}{2} erfc\left(\sqrt{\frac{A}{2}} - \sqrt{\frac{B}{2}}\right) + \frac{1}{2} erfc\left(\sqrt{\frac{A}{2}} + \sqrt{\frac{B}{2}}\right) - erfc\left(\sqrt{\frac{A}{2}}\right) , \quad (19)$$

The first term in (18) only depends on the signal to thermal noise ratio at the receiver input, while the second one accounts for MUI. The proposed approach was demonstrated to guarantee high accuracy in estimating receiver performance for impulse-based transmissions, even in the presence of scarcely populated systems, systems with dominating interferers, or low-rate systems [11].

5. PERFORMANCE ANALYSIS

The (UWB)^2 protocol described in Section 2 was tested by simulation. Simulation results were averaged over L different simulation runs. In each simulation run, N nodes were randomly located inside a square region with area A. Next, a realization of the channel impulse response, path loss, and delay spread was generated for each pair of nodes, with characteristics depending on the considered propagation scenario. These quantities were used by the interference module for introducing errors on the received packets, according to the MUI model described in Section 4.2.

We considered the scenarios CM1, CM2, CM5, and CM6 defined within IEEE 802.15.4a, corresponding to indoor propagation in residential environments in LOS and NLOS conditions, and outdoor propagation in LOS and NLOS [10]. CM1, CM2, CM5, and CM6 channels will be indicated as Scenarios 1, 2, 3, and 4, respectively. The settings for the path loss at a reference distance and path loss exponent in the four channel scenarios are presented in Table I.

Scenario	Path Loss @ d=1m	Path Loss exponent
1	43.9 dB	1.79
2	48.7 dB	4.58
3	43.29 dB	1.76
4	43.29 dB	2.5

TABLE 1: CHANNEL SCENARIOS CHARACTERISTICS.

During all simulations, the maximum size of 1288 bits was adopted for the PHYPDU. This value was obtained by considering as PHY payload a full size MACPDU of 129 bytes coded with a Reed Solomon (43,51) Forward Error Correction code in compliance with the specifications for the UWB PHY of the future 802.15.4a standard [12]. The 1224 coded bits were then combined with a PHY synchronization trailer of length 64 bits, leading to a size of 1288 bits for each PHYPDU.
Table II presents the main simulation settings.

Parameter	Setting
L	10
Number of nodes	From 10 to 20
Area	10 m × 10 m (Indoor) 50 m × 50 m (Outdoor)
Network topology	Random node positions
Channel model	See eq. (2) and [10]
User bit rate R	From 10 kb/s to 30 kb/s
Transmission rate	966 kb/s
Power	36.5 µW (FCC limit for Bandwidth ≅ 0.5 GHz)
Packet traffic model	Poisson generation process, uniform distribution for destination node
DATA packet length	1224 bits (+ 64 bits for Sync trailer)
Interference Model	Pulse Collision (see section 4)
Physical layer settings	N_S = 4, T_S = 258.8 ns T_m = 2 ns, Reed Solomon (43,51) FEC

TABLE 2: SIMULATION SETTING.

Performance of (UWB)^2 was analyzed as a function of:

- channel characteristics (indoor vs outdoor)
- number of terminals
- user bit rate
- access strategy (pure vs. slotted).

The comparison between pure and slotted Aloha was motivated by the fact that, as well known, in narrowband networks, slotted Aloha guarantees a higher (up to two times) throughput with respect to pure Aloha, thanks to a lower probability of packet collision. Our goal was to verify if this large performance gap is also present in low bit rate UWB networks, where the negative impact of packet collisions is mitigated by the high processing gain.

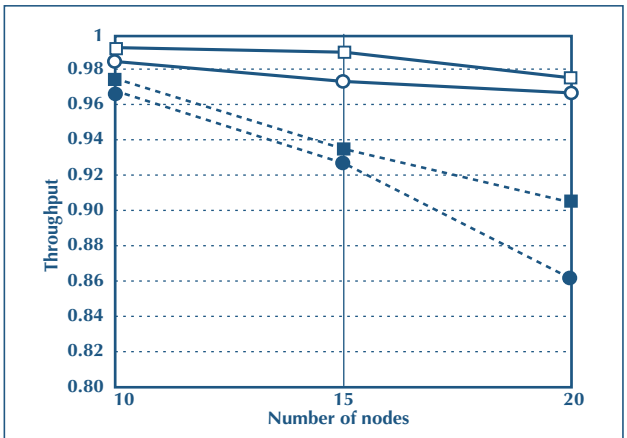

Figure 1: Throughput as a function of number of nodes for a user data rate R = 10 kb/s and Pure Aloha access (Filled line with white circles: Scenario 1 (Indoor LOS); Dashed line with full circles: Scenario 2 (Indoor NLOS); Filled line with white squares: Scenario 3 (Outdoor LOS); Dashed line with full squares: Scenario 4 (Outdoor NLOS).)

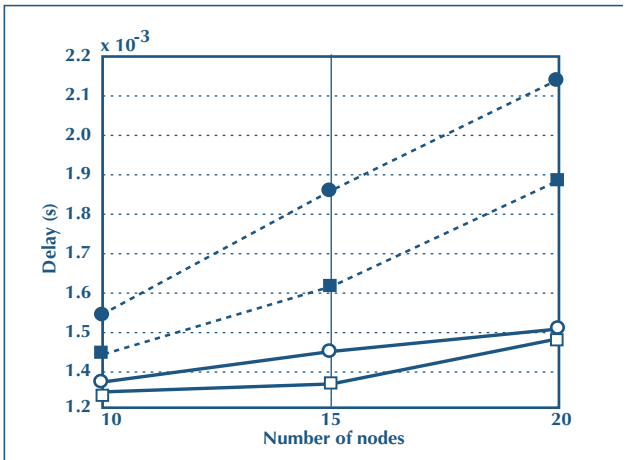

Figure 2: Delay as a function of number of nodes for a user data rate R = 10 kb/s and Pure Aloha access (Filled line with white circles: Scenario 1 (Indoor LOS); Dashed line with full circles: Scenario 2 (Indoor NLOS); Filled line with white squares: Scenario 3 (Outdoor LOS); Dashed line with full squares: Scenario 4 (Outdoor NLOS).)

Fig. 1 presents the throughput for the Pure Aloha strategy as a function of the number of nodes, for a user bit rate R = 10 kb/s.

Fig. 1 shows that in all cases throughput is greater than around 98% for both indoor and outdoor LOS scenarios and stays above 85%, even in NLOS conditions, where the higher path loss and the larger channel delay spread have a stronger impact on network performance.

Fig. 2 shows the delay measured in the same simulations, taking into account both the DATA PDU transmission time, equal to 1.33 ms, and the additional delay introduced by retransmissions following PDU collisions. Fig. 2 shows that for LOS scenarios the delay experienced by DATA PDUs is close to a minimum possible value, given by the DATA PDU transmission time. NLOS scenarios lead to a larger delay that is, however, below 2.2 ms in all cases.

Figs.3 and 4 show throughput and delay in the case of Slotted Aloha.

Fig.3 shows that Slotted Aloha leads to throughputs comparable to Pure Aloha, with values above 96% in LOS conditions and above 85% in the NLOS case.

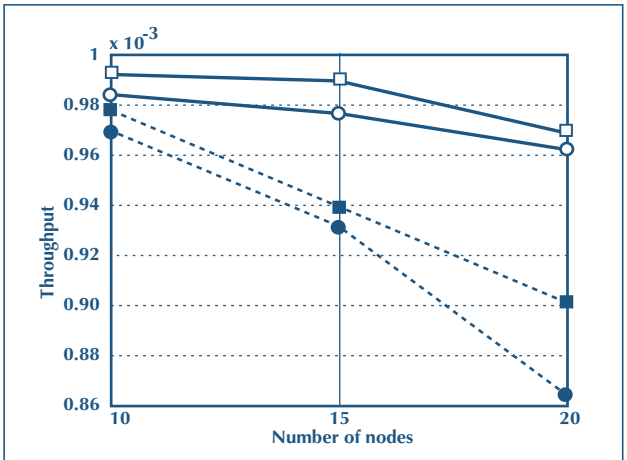

Figure 3: Throughput as a function of number of nodes for a user data rate R = 10 kb/s and Slotted Aloha access (Filled line with white circles: Scenario 1 (Indoor LOS); Dashed line with full circles: Scenario 2 (Indoor NLOS); Filled line with white squares: Scenario 3 (Outdoor LOS); Dashed line with full squares: Scenario 4 (Outdoor NLOS).)

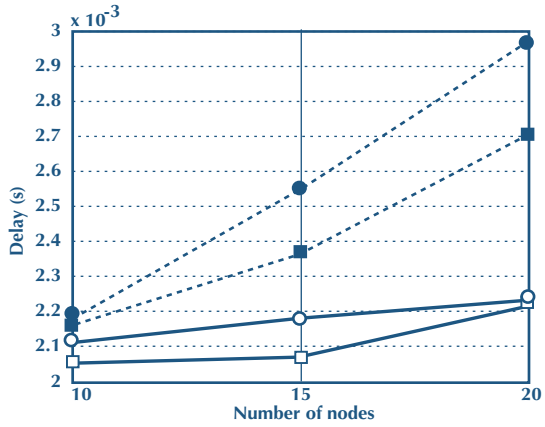

FIGURE 4: DELAY AS A FUNCTION OF NUMBER OF NODES FOR A USER DATA RATE R = 10 KB/S AND SLOTTED ALOHA ACCESS (FILLED LINE WITH WHITE CIRCLES: SCENARIO 1 (INDOOR LOS); DASHED LINE WITH FULL CIRCLES: SCENARIO 2 (INDOOR NLOS); FILLED LINE WITH WHITE SQUARES: SCENARIO 3 (OUTDOOR LOS); DASHED LINE WITH FULL SQUARES: SCENARIO 4 (OUTDOOR NLOS).)

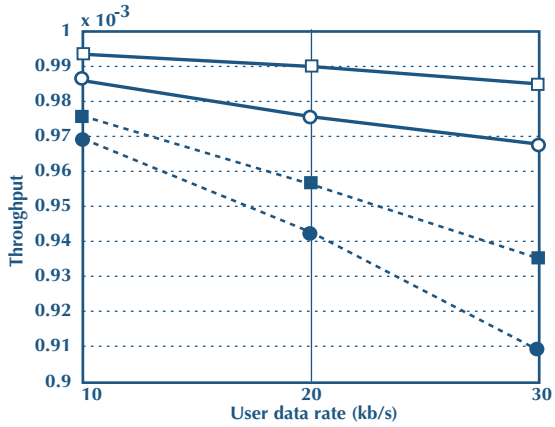

FIGURE 5: THROUGHPUT AS A FUNCTION OF USER DATA RATE FOR A NETWORK OF 10 NODES AND PURE ALOHA ACCESS (FILLED LINE WITH WHITE CIRCLES: SCENARIO 1 (INDOOR LOS); DASHED LINE WITH FULL CIRCLES: SCENARIO 2 (INDOOR NLOS); FILLED LINE WITH WHITE SQUARES: SCENARIO 3 (OUTDOOR LOS); DASHED LINE WITH FULL SQUARES: SCENARIO 4 (OUTDOOR NLOS).)

On the other hand, the additional delay in PDU transmission introduced by the slotted time axis leads to higher delays, in agreement with [7], as shown in Fig. 4.

Note, however, that the increase in the delay as a function of the number of users is slower than that in the delay for Pure Aloha, indicating that, for higher numbers of users, the Slotted Aloha approach should eventually guarantee lower delays and thus better performance.

In a second set of simulations, we evaluated the impact of the user data rate R on performance. We considered a network of 10 nodes and measured throughput and delay for three different data rates: 10, 20, and 30 kb/s, respectively.

The throughput obtained in the case of the Pure Aloha approach is presented in Fig. 5.

Fig. 5 shows that performance of the $(UWB)^2$ degrades gracefully as the offered traffic increases: the throughput is above 90% in all considered cases, and is well above 95% for the LOS scenarios. This behavior is confirmed by data on delay, as shown in Fig. 6. LOS scenarios have very low delays, and delays for NLOS scenarios are below 1.75 ms in all cases.

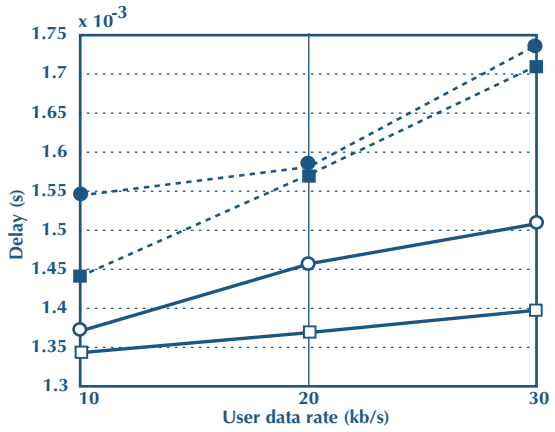

FIGURE 6: DELAY AS A FUNCTION OF USER DATA RATE FOR A NETWORK OF 10 NODES AND PURE ALOHA ACCESS (FILLED LINE WITH WHITE CIRCLES: SCENARIO 1 (INDOOR LOS); DASHED LINE WITH FULL CIRCLES: SCENARIO 2 (INDOOR NLOS); FILLED LINE WITH WHITE SQUARES: SCENARIO 3 (OUTDOOR LOS); DASHED LINE WITH FULL SQUARES: SCENARIO 4 (OUTDOOR NLOS).)

We measured throughput and delay for Slotted Aloha, presented in Figs 7 and 8, respectively.

Fig. 7 shows that Slotted Aloha provides slightly better results compared to Pure Aloha for high offered traffic loads, thanks to a lower probability of packet collision. The difference is more pronounced for NLOS scenarios, where Slotted Aloha

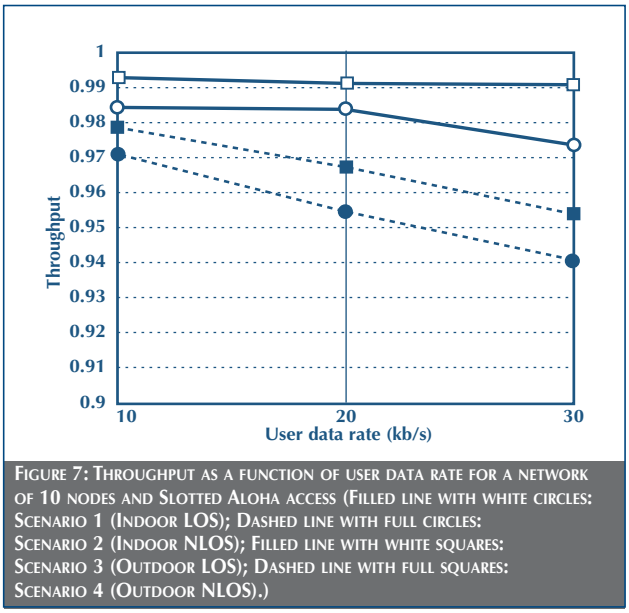

FIGURE 7: THROUGHPUT AS A FUNCTION OF USER DATA RATE FOR A NETWORK OF 10 NODES AND SLOTTED ALOHA ACCESS (FILLED LINE WITH WHITE CIRCLES: SCENARIO 1 (INDOOR LOS); DASHED LINE WITH FULL CIRCLES: SCENARIO 2 (INDOOR NLOS); FILLED LINE WITH WHITE SQUARES: SCENARIO 3 (OUTDOOR LOS); DASHED LINE WITH FULL SQUARES: SCENARIO 4 (OUTDOOR NLOS).)

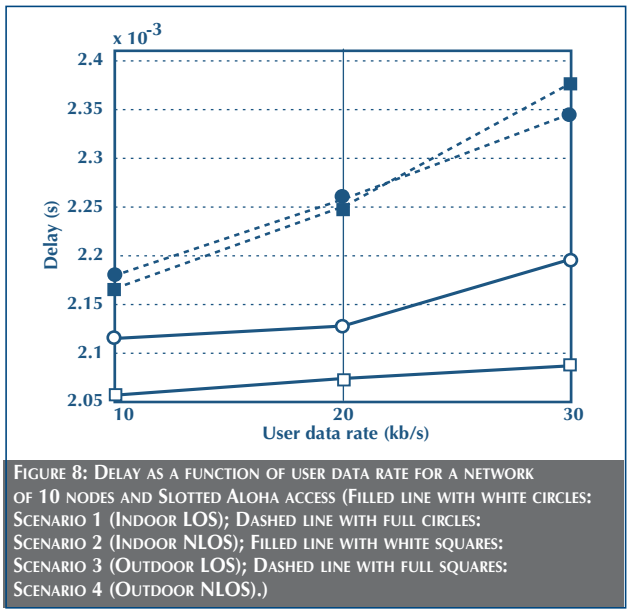

FIGURE 8: DELAY AS A FUNCTION OF USER DATA RATE FOR A NETWORK OF 10 NODES AND SLOTTED ALOHA ACCESS (FILLED LINE WITH WHITE CIRCLES: SCENARIO 1 (INDOOR LOS); DASHED LINE WITH FULL CIRCLES: SCENARIO 2 (INDOOR NLOS); FILLED LINE WITH WHITE SQUARES: SCENARIO 3 (OUTDOOR LOS); DASHED LINE WITH FULL SQUARES: SCENARIO 4 (OUTDOOR NLOS).)

guarantees in all cases a throughput higher than 94%, vs. 91% obtained by the Pure Aloha in the worst case.

The results are confirmed by Fig. 8, showing that the increase in delay as the offered traffic increases is proportionally lower than in the case of Pure Aloha, as a consequence of the higher robustness of the Slotted Aloha approach in high traffic scenarios.

6. CONCLUSIONS

In this work, the (UWB)^2 MAC protocol, originally introduced in [6], was revisited in view of its application to the future IEEE 802.15.4a standard. The structure of both control and DATA MACPDUs of the (UWB)^2 protocol was derived from the PDU structure of the existing 802.15.4 MAC, thus guaranteeing full support for the network topologies defined within the original standard. The (UWB)^2 protocol adopts Aloha for medium access and CDMA for multiple access, based on the use of Time Hopping codes. The protocol can operate in either a slot-free (pure) or a slotted fashion, and can thus fit both centralized and distributed network architectures. The protocol also includes a ranging procedure in order to enable the operation of location-based protocols at higher layers.

The performance of the (UWB)^2 MAC was evaluated in the presence of multipath-affected propagation channels, derived from the channel model proposed within the IEEE 802.15.4a Task Group. Performance in both pure and slotted modes of operation was analyzed by simulation in indoor and outdoor scenarios in both Line-Of-Sight and Non-Line-Of-Sight conditions. In order to properly take into account the impact of multipath and channel delay spread on network performance, we also introduced an ad-hoc MUI model based on the concept of Pulse Collision in this work.

Simulation results show that the (UWB)^2 MAC guarantees satisfactory network performance in both indoor and outdoor scenarios, even in presence of NLOS propagation conditions. Furthermore, network performance in case of high traffic loads can be improved by adopting a Slotted Aloha approach. Results suggest that, despite its simplicity, the (UWB)^2 MAC provides high throughput and low delays for bit rates up to several tens of kb/s and for networks composed of tens of terminals, thereby making it a viable solution for future UWB low data rate networks.

ACKNOWLEDGMENTS

This work was partially supported by the European Union within the Integrated Projects n. 506897 - PULSERS and n. 511766 LIAISON and by STMicroelectronics Srl (Italy) within the research contract "UWB Ranging and Positioning in Radio Communication Systems."

REFERENCES

[1] The IEEE 802.15.4 standard, available at http://www.ieee.org.

[2] P. Kinney, "ZIGBEE TECHNOLOGY: WIRELESS CONTROL THAT SIMPLY WORKS," (2003), Available at http://www.zigbee.org/en/resources/#WhitePapers.

[3] IEEE 802.15.TG4a page, http://www.ieee802.org/15/pub/TG4a.html.

[4] M.-G. Di Benedetto and Giancola G., **Understanding Ultra Wide Band Radio fundamentals**, Prentice Hall, 2004.

[5] L. De Nardis and G. M. Maggio, "LOW DATA RATE UWB NETWORKS," in Ultra Wideband Wireless Communications, John Wiley & Sons, Inc. (May 2006).

[6] M.-G. Di Benedetto, L. De Nardis, M. Junk and G. Giancola, "$(UWB)^2$: UNCOORDINATED, WIRELESS, BASEBORN MEDIUM ACCESS FOR UWB COMMUNICATION NETWORKS," MONET: Special Issue on WLAN optimization at the MAC and network levels, vol. 5, no. 10, pp. 663-674, October 2005.

[7] L. De Nardis, G. Giancola and M.-G. Di Benedetto, "PERFORMANCE ANALYSIS OF UNCOORDINATED MEDIUM ACCESS CONTROL IN LOW DATA RATE UWB NETWORKS," in Proceedings of the 1st IEEE/CreateNet International Workshop on "ULTRAWIDEBAND WIRELESS NETWORKING," within the 2nd International Conference on Broadband Networks, (invited paper), pp. 206-212, October 2005, Boston, Massachusetts, USA.

[8] L. De Nardis and M.-G. Di Benedetto, "MEDIUM ACCESS CONTROL DESIGN FOR UWB COMMUNICATION SYSTEMS: REVIEW AND TRENDS," KICS Journal of Communications and Networks, vol. 5, no. 4, pp. 386–393, December 2003.

[9] E. S. Sousa and J. A. Silvester, "SPREADING CODE PROTOCOLS FOR DISTRIBUTED SPREAD-SPECTRUM PACKET RADIO NETWORKS," IEEE Transactions on Communications, vol. COM–36, no. 3, pp. 272–281, March 1988.

[10] IEEE 802.15.4a Channel Model Final Report, Rev.1 (November 2004), available at: ftp://ieee:wireless@ftp.802wirelessworld.com/15/04/15-04-0662-00-004a-channel-model-final-report-r1.pdf.

[11] G. Giancola and M.-G. Di Benedetto, "A NOVEL APPROACH FOR ESTIMATING MULTI USER INTERFERENCE IN IMPULSE RADIO UWB NETWORKS: THE PULSE COLLISION MODEL," (invited paper) EURASIP Signal Processing Journal, Special Issue on Signal Processing in UWB Communications, vol. 86, no. 5, pp. 2172-2184, May 2006.

[12] G. M. Maggio, "802.15.4A UWB-PHY," IEEE 802.15.4a Document # IEEE 15-05-0707-01-004a, November 2005.

■ CONTACT: ST.JOURNAL@ST.COM ■